Influence of lattice volume on magnetic states of $Ce_2Fe_{16}MnD_y$ compounds ($y=0,1,2.3$)

O. Prokhnenko[a)]
Hahn Meitner Institute, Glienickerstrasse 100, 14109 Berlin, Germany and Institute of Physics AS CR, Na Slovance 2, 182 21 Prague 8, Czech Republic

Z. Arnold
Institute of Physics AS CR, Na Slovance 2, 182 21 Prague 8, Czech Republic

A. Kuchin
Institute for Metal Physics, S. Kovalevskaya 18, Ekaterinburg, 620219 Russia

C. Ritter
Institute Laue Langevin, BP 156, 38042 Grenoble Cedex 9, France

O. Isnard
Laboratoire de Cristallographie, CNRS, Université J. Fourier, BP 166, 38042 Grenoble, Cedex 9, France

J. Kamarád
Institute of Physics AS CR, Na Slovance 2, 182 21 Prague 8, Czech Republic

W. Iwasieczko and H. Drulis
Polish Academy of Science, Trzebiatowski Institute of Low Temperature and Structure Research, 59-950 Wroclaw 2, P.O. Box 1410, Poland

(Received 2 February 2006; accepted 8 April 2006; published online 5 July 2006)

The substitution of Mn for Fe in Ce_2Fe_{17} suppresses its ferromagnetic ground state completely for Mn contents $x \geqslant 0.5$ Mn/f.u. $Ce_2Fe_{16}Mn$ has only an antiferromagnetic phase (incommensurate helix along c axis) below $T_N=198$ K. In this paper, we present and discuss the effects of deuterium insertion (that can be considered as an application of negative chemical pressure) on the magnetostructural properties of $Ce_2Fe_{16}Mn$. Application of (positive) high pressures up to 10 kbar on $Ce_2Fe_{16}MnD_y$ deuterides ($y=1,2.3$) allowed us to estimate the role of lattice volume and to divide it from the role of modified electronic band structure that both determines the magnetic states of the deuterated compounds. The results show that a ferromagnetic phase is stabilized by the insertion of D into the antiferromagnetic $Ce_2Fe_{16}Mn$. The Curie temperature T_C of $Ce_2Fe_{16}MnD_y$ deuterides increases with increasing D content reaching $T_C=258$ K for $y=2.3$ and remarkably decreases with pressure $dT_C/dP=-5.4$ K/kbar and $dT_C/dP=-3.6$ K/kbar for $Ce_2Fe_{16}MnD_1$ and $Ce_2Fe_{16}MnD_{2.3}$, respectively. Significant difference between the magnetization of $Ce_2Fe_{16}MnD_1$ under pressure and the one of the parent compound at ambient pressure indicates that changes of the volume alone cannot determine the magnetic states upon the initial deuteration. However, the volume expansion becomes dominant when increasing the deuterium content up to 2.3 D/f.u.
 [DOI: 10.1063/1.2208290]

I. INTRODUCTION

The magnetic phase diagram of $Ce_2Fe_{17-x}Mn_x$ ($0 \leqslant x \leqslant 2$) is rich and rather unusual for rare earth transition metal intermetallic compounds. Whereas $R_2Fe_{17-x}Mn_x$ compounds with $R=$Y, Pr, Nd, Sm, Gd, Tb, Er show only a monotonous decrease of both the magnetization and the Curie temperature with increasing Mn content as a result of an antiparallel coupling between Fe and Mn moments,[1–7] the case of $R=$Ce is unique. Binary Ce_2Fe_{17} has a collinear ferromagnetic (FM) phase below $\sim$100 K, an antiferromagnetic (AFM) phase between 100 K and $T_N \sim 210$ K and a paramagnetic state above T_N. The transition from the FM to the AFM state was described in the framework of the Bethe-Slater model [see, e.g., Ref. 8] and attributed to the increase of the negative exchange interactions between Fe magnetic moments on four different magnetic sites caused by the anomalous negative thermal expansion along the c axis of the rhombohedral (R-3m) crystal structure.[9] An extraordinary sensitivity of the ferromagnetic state of Ce_2Fe_{17} to the decrease of volume was confirmed by the magnetization and neutron diffraction measurements under pressure.[10,11] Both showed that a decrease of the volume leads to the suppression of the FM ground state and its substitution by the AFM one.

The situation gets even more complicated by the substitution of Mn for Fe which leads to changes in the electronic band structure, changes of interatomic distances and has a strong preferential character. Mn occupies mainly dumbbell 6c site and avoids 9d site whereas 18f and 18h sites are occupied almost equally.[12] The effect of the substitution on the magnetic properties can be divided in two parts. For

[a)]Electronic mail: prokhnenko@hmi.de

small Mn contents, the temperature stability range of the FM ground state gets narrowed and suppressed completely when $x=0.5$. $Ce_2Fe_{17-x}Mn_x$ compounds with $0.5 \leqslant x < 1.3$ have only an AFM phase below $T_N \sim 200$ K. Further increase of the Mn content ($1.3 \leqslant x < 2$) leads to the reentrance of a FM phase at low temperatures. Over the whole Mn-concentration range the magnetization decreases with increasing Mn content.[12]

The disappearance of the ferromagnetism in AFM $Ce_2Fe_{17-x}Mn_x$ compounds ($0.5 \leqslant x < 1.3$) cannot be entirely explained in the way it has been done for the binary compound. According to Ref. 12 the lattice (both *a* and *c* parameters) first expands upon Mn substitution for $0 \leqslant x \leqslant 0.9$, then slightly contracts for $0.9 < x \leqslant 1.3$ but always stays larger than the binary one. This implies that in addition to the effect based on the changes of interatomic distances resulting from the different atomic radius of the Mn atom, the changes of the electronic band structure in the vicinity of the Fermi level might play an important role in determining the magnetic properties of $Ce_2Fe_{17-x}Mn_x$ compounds. In the case of Si and Al substitutions for Fe, the obtained change of the density of states at the Fermi level allowed us to explain consistently[13,14] the decrease of T_C for both $R_2Fe_{17-x}Si_x$ (lattice contraction)[15–17] and $R_2Fe_{17-x}Al_x$ (lattice expansion).[18]

In this paper, we have restricted ourselves to the compound $Ce_2Fe_{16}Mn$ as a typical representative of the AFM ($T_N=198$ K) $Ce_2Fe_{17-x}Mn_x$ compounds. Its magnetic structure can be presented as an incommensurate helix along the *c* axis of the rhombohedral structure with the propagation vector $\boldsymbol{\tau}=(0,0,0.378)$ and an average magnetic moment per transition metal site of $1.1\mu_B$. Application of high pressures (pure volume effect) results in a distortion of the helix so that an uncompensated ferromagnetic component appears in the basal plane giving the ferromagnetic response of the bulk magnetization.[19,20] As far as the main structural details of the pressure induced magnetic structure stay antiferromagnetic, one can expect the domination of the electronic band structure changes over the volume effects upon Mn for Fe substitution in $Ce_2Fe_{17-x}Mn_x$ with $0.5 \leqslant x < 1.3$.

Recently, magnetic measurements on hydrogenated $Ce_2Fe_{17-x}Mn_x$ compounds were reported. According to Refs. 21 and 22 $Ce_2Fe_{17-x}Mn_xH_y$ ($x=0.75,1$ and $y=1,2,3$) become ferromagnetic for $y \geqslant 2$. The magnetic state of the $Ce_2Fe_{17-x}Mn_xH_y$ compounds with $x=1$ and $y=1$ was either reported to stay unchanged[21] or to become of noncollinear ferromagnetic type for $Ce_2Fe_{17-x}Mn_xH_y$ compounds with $x=0.75,1$ and $y=1$.[22] The suppression of the AFM and the stabilization of the FM with hydrogenation were explained as being caused by the increase of the exchange integrals due to the volume expansion.[21] Similar conclusions were made for binary $Ce_2Fe_{17}H_y$ compounds, where magnetic properties were reported to be induced mainly by the increase of Fe–Fe interatomic distances.[23,24]

As far as hydrogen induced lattice expansion can be considered as application of negative chemical pressure, it is quite interesting to investigate the magnetic states developed in AFM $Ce_2Fe_{16}Mn$ after hydrogenation and to determine whether the suppression of the AFM and the creation of FM is a volume (lattice expansion) effect. For this reason we performed a number of neutron diffraction measurements at ambient pressure and magnetization measurements under high pressures up to 10 kbar. The first is aimed to determine the magnetic structures realized upon hydrogenation. The second should help us to divide magnetic phenomena induced by changes of volume from those induced by changes of the electronic band structure. As hydrogen is a strong incoherent neutron scatterer, all measurements were carried out on deuterated $Ce_2Fe_{16}MnD_y$ ($y=1,2.3$) samples.

II. EXPERIMENT

The polycrystalline $Ce_2Fe_{16}Mn$ compound was prepared by high-frequency melting under argon atmosphere in an Al_2O_3 crucible. The as-cast ingots were annealed under vacuum at 1000 K for 14 days. The deuterides $Ce_2Fe_{16}MnD_y$ with deuterium concentrations $y=1$ and 2.3 were prepared in a stainless steel reactor chamber of a conventional Sieverts-type volumetric system with starting deuterium pressure of 3 atm through the direct absorption of deuterium by the metal after a short thermal activation procedure at 250 °C. The samples were kept at this temperature for 48 h and then slowly cooled down to room temperature with a rate of about 20 °C/h. The deuterium concentration was determined by a volumetric method with an accuracy of ±0.02 deuterium atoms per formula unit. The sample quality was checked by X-ray diffraction at room temperature.

The temperature dependence of the low field ($H=50$ Oe) magnetization was measured in a superconducting quantum interference device (SQUID) magnetometer in the temperature range of 5–300 K at ambient pressure and under pressures up to 10 kbar. Measurements were performed in zero field cooling (ZFC) and field cooling (FC) runs where the external magnetic field was applied at the lowest and the highest temperatures, respectively. The field dependence of the isothermal magnetization was measured in magnetic fields up to 50 kOe. A miniature CuBe piston-cylinder high pressure cell filled with a mixture of mineral oils as a pressure transmitting medium was used for the pressure generation.[25] The actual pressure values for the isothermal magnetization curves were determined taking into account the temperature induced changes of the pressure inside the cell. For the temperature dependent measurements the given pressure value corresponds to the pressure value at 5 K.

Neutron diffraction measurements were carried out on powder $Ce_2Fe_{16}MnD_y$ samples in the temperature range of 2–300 K. The data were collected with the double-axis multicounter diffractometer D1B at the Institute Laue Langevin (Grenoble) using a wavelength of 2.52 Å. The stoichiometry of the compounds and the position of the inserted deuterium were determined at room temperature using the high resolution powder diffractometer D2B ($\lambda=1.596$ Å), as well at the ILL.

Neutron diffraction data analysis was done using the FULLPROF refinement package.[26]

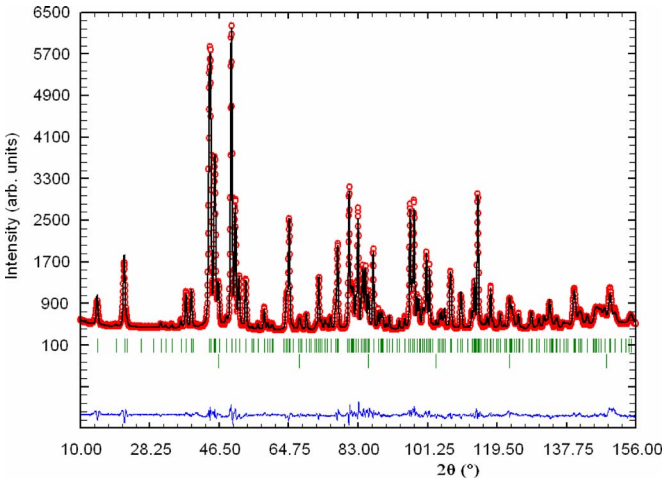

FIG. 1. (Color online) Observed (red), calculated (black), and difference (blue) neutron diffraction patterns of $Ce_2Fe_{16}MnD_1$ compound as measured with high resolution D2B diffractometer at room temperature.

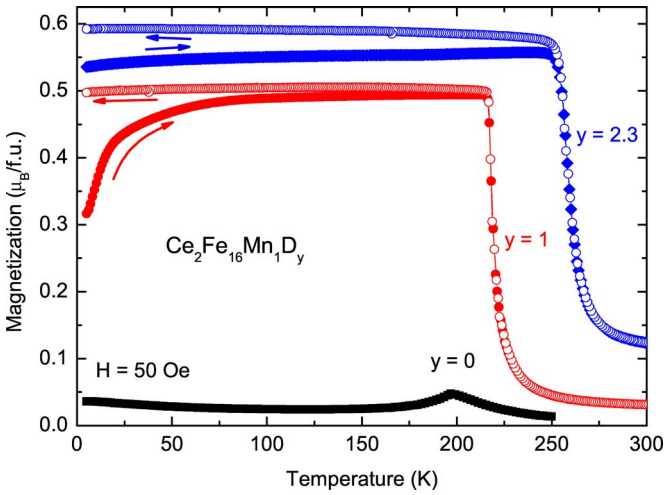

FIG. 2. (Color online) Temperature dependence of the magnetization of $Ce_2Fe_{16}MnD_y$ measured at $H=50$ Oe at ambient pressure. ZFC and FC runs are marked by solid and open symbols, respectively.

III. RESULTS AND DISCUSSION

A. Crystal structure

From the refinement of the high resolution neutron diffraction data we determined the crystal structure of the three studied $Ce_2Fe_{16}MnD_y$ compounds ($y=0,1,2.3$). A typical room temperature neutron diffraction pattern is shown in Fig. 1. In all cases the $Ce_2Fe_{16}MnD_y$ compounds crystallize in the rhombohedral (R-3m) Th_2Zn_{17}-type crystal structure typical for R_2Fe_{17} with light rare earth elements.[27] The rhombohedral triple unit cell consists of three formula units. This structure can be considered as a natural multilayer structure where the atomic layers are stacked along in c direction. The Fe atoms are located in four (6c, 9d, 18f, and 18h) inequivalent atomic positions. Structural details are presented in Table I. The D atoms are located on the 9e site in agreement with earlier investigation on isotype $Ce_2Fe_{17}H_y$ compounds.[23,28] For this deuterium concentration $y \leqslant 3$, the D atoms do not fill the tetrahedral interstitial sites thus confirming that the octahedral site is more favorable as shown previously.[23,29] Such a location of deuterium atoms leads to the expansion of the lattice mainly in a direction, leaving the c parameter only slightly varying (even decreasing) with D content (Table I). Similar effects were obtained in $Ce_2Fe_{17}H_y$ and $Ce_2Fe_{17-x}Mn_xH_y$ hydrides.[21–23,28,29]

B. Magnetic properties at ambient pressure

The magnetization measurements shown in Fig. 2 confirm that the introduction of D favors a ferromagnetic state in $Ce_2Fe_{16}MnD_y$ ($y=1,2.3$). Indeed, while the temperature dependence of the low field magnetization of the parent $Ce_2Fe_{16}Mn$ sample shows a behavior typical for antiferromagnets with a peak at the Néel temperature $T_N=198$ K, the deuterated samples show a rather ferromagnetic behavior: they exhibit spontaneous magnetizations below $T_C=218$ K

TABLE I. Structural parameters of $Ce_2Fe_{16}MnD_y$ compounds at room temperature.

	$Ce_2Fe_{16}MnD_y$		
Structural parameters	$y=0$	$y=1$	$y=2.3$
a (Å)	8.497(1)	8.533(1)	8.575(1)
c (Å)	12.417(2)	12.407(2)	12.410(2)
V (Å^3)	776.4	782.35	790.26
Ce, 6c: (0;0;z)	0.344(4)	0.346(3)	0.345(2)
Fe/Mn, 6c: (0;0;z)	0.097(2)	0.097(2)	0.098(1)
[Fe/Mn occupation]	[0.133(1)/0.034(1)]	[0.134(1)/0.033(1)]	[0.137(1)/0.030(1)]
Fe/Mn, 18f: (x;0;0)	0.290(1)	0.287(1)	0.285(1)
[Fe/Mn occupation]	[0.472(1)/0.028(1)]	[0.458(3)/0.042(3)]	[0.467(2)/0.033(2)]
Fe/Mn, 18h: (x;−x;z)	0.502(1); 0.498(1); 0.155(1)	0.502(1); 0.498(1); 0.155(1)	0.502(1); 0.498(1) 0.155(1)
[Fe/Mn occupation]	[0.478(1)/0.022(1)]	[0.475(3)/0.025(3)]	[0.482(2)/0.018(2)]
Fe, 9d: (1/2;0;1/2)	⋯	⋯	⋯
D, 9e: (1/2;0;0)	⋯	⋯	⋯
R_{Bragg} (%)	4.77	5.50	3.99
χ^2	3.52	3.29	2.72
Calculated D content	⋯	0.992(3)	2.209(3)

and T_C=258 K for $Ce_2Fe_{16}MnD_1$ and $Ce_2Fe_{16}MnD_{2.3}$, respectively. Both magnetization curves have steplike anomalies as the samples undergo transitions to the ordered magnetic state. Below the transition temperatures (determined as the inflection points of the corresponding curves), the magnetization stays almost constant except for $Ce_2Fe_{16}MnD_1$ when zero field cooled. Applying a small magnetic field of 50 Oe at low temperatures, the magnetization of $Ce_2Fe_{16}MnD_1$ is first low, then it increases abruptly up to 15 K. Above this temperature the magnetization curve shows a wide knee increasing slowly and becoming flat only above 100 K. This effect is field and history dependent, it cannot be observed for the FC run (Fig. 2). This indicates that the ground state of $Ce_2Fe_{16}MnD_1$ is not purely ferromagnetic. The ferromagnetism, however, can be easily induced by a small magnetic field or by increasing temperature. The magnetization curves of $Ce_2Fe_{16}MnD_{2.3}$ show only minor differences between the FC and ZFC runs.

If we compare these results on $Ce_2Fe_{16}MnD_1$ with the previously published results obtained on $Ce_2Fe_{16}MnH_1$,[21] strong differences are found. One can, however, realize that the magnetic behavior of $Ce_2Fe_{16}MnH_1$ as presented in Ref. 21 shows a surprisingly similar magnetic behavior as the parent compound $Ce_2Fe_{16}Mn$: the same value of T_N, and just a higher magnetization. In our opinion this result has to be connected to an inhomogeneity of the Ref. 21 studied hydride where the form of the obtained magnetization curve might be simply caused by a superposition of signals coming from a mixture of $Ce_2Fe_{16}Mn$ and $Ce_2Fe_{16}MnH_1$ phases. One of our first deuterides $Ce_2Fe_{16}MnD_1$ had shown a similar behavior of the magnetization: the high resolution neutron diffraction data showed in the following that the sample could not be refined as a single phase. The authors of Ref. 22 proposed a magnetically inhomogeneous state in $Ce_2Fe_{16.25}Mn_{0.75}H$ (caused by an inhomogeneous distribution of hydrogen among the interstitial sites) in order to describe their magnetization data. We want to recall here that the refinement of the high resolution neutron diffraction data gives us the certainty of having single phase homogeneous $Ce_2Fe_{16}MnD_y$ compounds.

Figure 3 shows that the magnetization isotherms of $Ce_2Fe_{16}MnD_1$ and $Ce_2Fe_{16}MnD_{2.3}$ significantly differ from that of $Ce_2Fe_{16}Mn$. The last has a pronounced metamagnetic transition at about 3 kOe which is absent in the deuterated samples. $Ce_2Fe_{16}MnD_1$ and $Ce_2Fe_{16}MnD_{2.3}$ have similar magnetization curves showing spontaneous magnetization, which increases with the introduction of deuterium. Detailed analyses of the low field curves measured at different temperatures showed, however, a very weak (critical field is ~200 Oe) metamagnetic transitions present as well in $Ce_2Fe_{16}MnD_1$ at temperatures below 50 K. This result is in agreement with the M vs T dependence (Fig. 2) and confirms that the ground state of $Ce_2Fe_{16}MnD_1$ is not ferromagnetic.

C. Neutron diffraction

The thermal evolution of the low angle parts of the neutron diffraction patterns of $Ce_2Fe_{16}MnD_y$ (y=0,1,2.3) is shown in form of an contour plots in Fig. 4. The magnetic

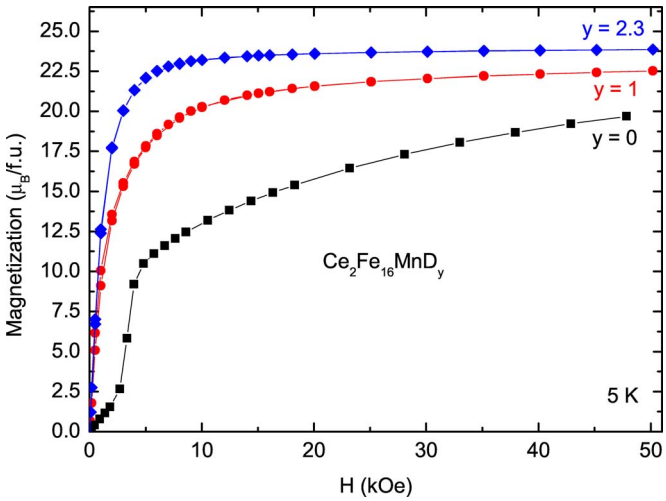

FIG. 3. (Color online) Magnetization isotherms of $Ce_2Fe_{16}MnD_y$ at 5 K and ambient pressure.

structure of the parent compound $Ce_2Fe_{16}Mn$ has been already reported,[20] it is a helix with an incommensurate propagation vector along c axis $\boldsymbol{\tau}$=(0,0,0.378). Figures 4(a) and 4(b) show the incommensurate $(000)^+$ magnetic satellite appearing below T_N at 2θ=4.5° and the (101) nuclear reflection which has no magnetic contribution within the whole temperature range.

The introduction of one D atom leads to crucial changes in the diffraction pattern [Figs. 4(c) and 4(d)]. First of all, a broad peak appears in $Ce_2Fe_{16}MnD_1$ at elevated temperatures at $2\theta \approx 2.2°$. The intensity of this peak increases with decreasing temperature and reaches a maximum at about 220 K, which coincides with T_C of this compound. Further cooling leads to the gradual decrease of its intensity and a simultaneous appearance of a magnetic contribution on top of the nuclear (101) reflection. The magnetic contribution to (101) is the largest at intermediate temperatures (180–80 K). At temperatures below 60 K, however, the intensity of (101) goes down again and recovers the paramagnetic value below 40 K. At the same time magnetic peaks appear below ~110 K on the left side of the (101) reflection and at low angles. The later grows from the tail of the earlier described broad peak shifting to a lower angle position.

The temperature dependence of the observed peculiarities is in perfect agreement with the magnetic measurements and explains the magnetization behavior of the compound. The broad peak at $2\theta \approx 2.2°$ corresponds to the critical scattering appearing in systems close to a phase transition. The presence of this peak at room temperature and its increase up to T_C indicate the growth of magnetic short range order (SRO) regions in the sample. The position of the peak (incommensurate or superlattice with $\tau_z \sim 1/5$) indicates that the magnetic interactions above T_C are of negative character. Most probably there are competitions between negative and positive exchange interactions because the positive ones start to dominate below T_C. The regions of magnetic SRO get smaller (but do not vanish completely below the ordering temperature), and the increase of the nuclear intensities indicate the onset of the ferromagnetic order already seen in the magnetization curve. This, actually, means that the magnetic

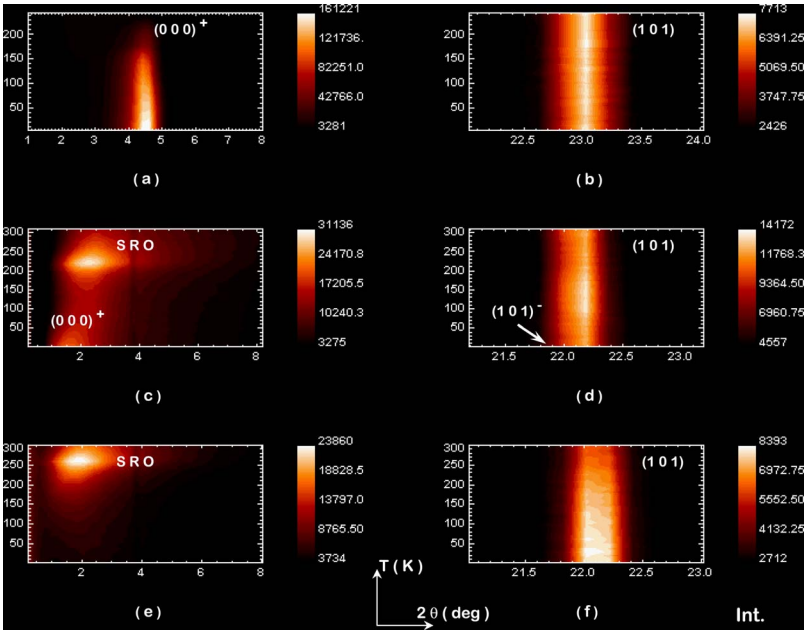

FIG. 4. (Color online) Temperature evolution of the neutron diffraction pattern of $Ce_2Fe_{16}MnD_y$ measured with D1B diffractometer. (a), (c), and (e) low angle contour plots showing the temperature dependences of the magnetic SRO and $(000)^+$ satellite for y=0, 1, and 2.3, respectively. (b), (d), and (f) contour plots showing the temperature dependence of the nuclear (101) reflection and the magnetic $(101)^-$ satellite for $y=0$, 1, and 2.3, respectively.

state at intermediate temperatures involves long range FM order and decreasing short range AFM clusters. The refinement of the neutron diffraction data at 130 K shows that the Fe(Mn) magnetic moments are aligned parallel in the basal plane. The average moment per site amounts to $(1.36\pm0.07)\mu_B$ which is in good agreement with $1.26\mu_B$ obtained from the magnetization at 50 kOe (Fig. 3).

Below 100 K, however, a reverse process takes place. The negative exchange interactions dominating in SRO clusters get obviously enhanced to a point that the long range FM is transformed into long range AFM. The last is characterized by $(000)^+$ and $(101)^-$ magnetic satellites observed below 100 K. The propagation vector is estimated to be very small, $\tau<0.011$ Å^{-1}, at 2 K. Unfortunately, this does not allow us to make a quantitative determination of the magnetic structure. However, from the magnetic peaks present, we can expect a similar type of structure as found for the parent compound where τ_z would be less than 0.137 r.l.u. (reciprocal lattice units). The presence of a FM-AFM transition explains the decrease of the low field magnetization below 100 K (Fig. 2). The very low value of the propagation vector indicates that the period of the magnetic structure is very large (angle between moments in neighboring atomic layers is small), i.e., it explains the very low value of the field needed for the metamagnetic transition into the forced FM state observed in the magnetization measurements.

It is worth emphasizing that the introduction of only 1 D/f.u. is enough to drive the system ferromagnetic. The final (AFM) ground state is very unstable, and small external fields or a further introduction of D easily suppresses it. Evidencing the (AFM) ground state was only possible using neutron diffraction and low field magnetization measurements (ZFC). According to Refs. 21 and 22 the M vs T characterization of hydrides was normally performed in a FC regime. This should be the reason why no decrease of the magnetization was observed at low temperatures.

Further insertion of D leads to the stabilization of the FM state down to the lowest temperatures. As before, the neutron diffraction patterns of $Ce_2Fe_{16}MnD_{2.3}$ [Figs. 4(e) and 4(f)] show the increase of nuclear intensities below T_C indicating the onset of FM order, the transition being preceded by a broad peak of critical magnetic scattering at $2\theta\approx2°$. The magnetic contribution on top of the nuclear reflections appears at $T_C=260$ K and exists down to 2 K contrary to $Ce_2Fe_{16}MnD_1$ compound. Refinement of the neutron diffraction data at 2 K gives a ferromagnetic arrangement of Fe(Mn) magnetic moments in the basal plane. The average moment per site equals to $(1.72\pm0.05)\mu_B$ slightly higher than the $1.4\mu_B$ obtained from the magnetization measurements (Fig. 3).

Similarly to $Ce_2Fe_{16}MnD_1$, the SRO peak with a maximum at ~260 K shows the presence of SRO regions with dominating negative exchange interactions. Interesting is the fact that the tail of this SRO peak exists far below T_C down practically to the lowest temperatures. This indicates that the magnetic state of $Ce_2Fe_{16}MnD_{2.3}$ again involves the coexistence of long range FM order and short range AFM clusters. This fact is reflected in the slightly different temperature dependences of the magnetization for ZFC and FC runs.

Finally, we report the thermal behavior of the lattice of the $Ce_2Fe_{16}MnD_y$ compounds ($y=0,1,2.3$). Figure 5 shows that the temperature dependence of the lattice parameters of all compounds is highly anisotropic, while the lattice contracts in a direction on cooling it expands at the same time anomalously in c direction. The observed expansion in c direction is present in $Ce_2Fe_{16}Mn$ at all temperatures below room temperature, in $Ce_2Fe_{16}MnD_1$ and $Ce_2Fe_{16}MnD_{2.3}$ only below T_C. A negative thermal expansion is very typical for $Ce_2Fe_{17-x}Mn_x$ ($0\leqslant x<2$) (Refs. 20 and 30–32) and R_2Fe_{17} with nonmagnetic R=Lu and Y.[33] In all mentioned compounds the thermal expansion is negative below ordering temperatures. A typical paramagnetic thermal expansion based on the lattice contribution is observed in Y_2Fe_{17} (T_C ~310 K) and Lu_2Fe_{17} (T_N~270 K) above 500 K only.[33] This behavior was connected to the presence of short range

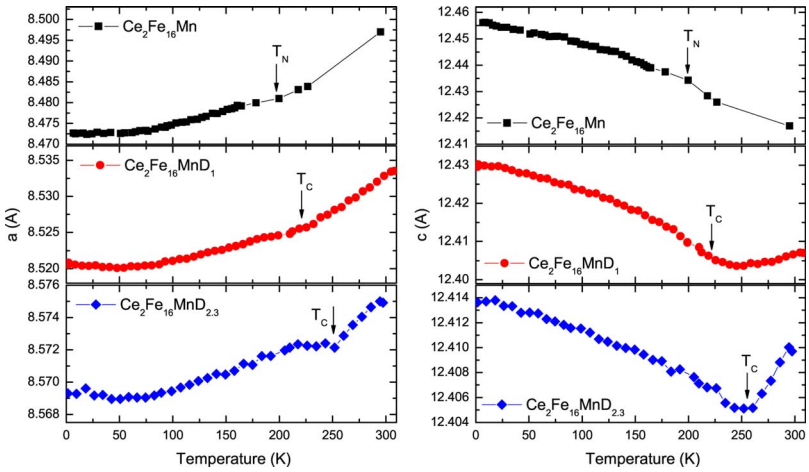

FIG. 5. (Color online) Temperature dependence of *a*- and *c*-lattice parameters of $Ce_2Fe_{16}MnD_y$ compounds ($y=0,1,2.3$).

magnetic ordering existing far above T_C or T_N. Inverting the same argumentation this would mean in the case of our deuterides that short range magnetic ordering appears close to T_C only. This is exactly what was found in the neutron diffraction data where the pronounced SRO peak appears only in vicinity of T_C (Fig. 4).

In the case of the binary Y_2Fe_{17}, Ce_2Fe_{17}, and Lu_2Fe_{17} the increase of the *c* parameter with decreasing temperature was able to explain (in terms of the Bethe-Slater model) the different FM-AFM (and AFM-FM) transitions induced by *T* or *P*.[34] This, however, does not hold for the Mn substituted and deuterated compounds as $Ce_2Fe_{16}Mn$ with the biggest *c* at low temperatures is AFM and $Ce_2Fe_{16}MnD_{2.3}$ with the smallest *c* at low temperatures is FM. This points strongly to the conclusion that the negative thermal expansion along the *c* axis cannot be the dominating factor determining the magnetic states of the $Ce_2Fe_{16}MnD_y$ compounds ($y=0,1,2.3$).

The temperature behavior of the *a* parameters does not show the same pronounced magnetic anomalies as the *c* parameters. A change of slope is visible below the ordering temperatures in $Ce_2Fe_{16}Mn$ and $Ce_2Fe_{16}MnD_1$ while a plateau around T_C is present in $Ce_2Fe_{16}MnD_{2.3}$. The slope change around ordering temperatures in *a* vs *T* dependences is also typical for R_2Fe_{17} with nonmagnetic Y and Lu.[33]

The increase of the *a* parameter and of the volume in general upon Mn for Fe substitution in Ce_2Fe_{17} and upon D insertion in $Ce_2Fe_{16}Mn$ leads to opposite results, suppression of FM and induction of AFM in $Ce_2Fe_{16}Mn$ and suppression of AFM and induction of FM in $Ce_2Fe_{16}MnD_y$ compounds ($y=1,2.3$). This indicates that the increase of the *a* parameter cannot also describe the observed phenomena. Thus, one can suppose that the changes of the electronic band structure play a crucial role in the magnetism of $Ce_2Fe_{16}MnD_y$ compounds ($y=0,1,2.3$).

D. Magnetic properties under high pressure

Magnetization measurements were performed as a function of pressure in order to distinguish further between the two factors which contribute in determining the magnetic states of $Ce_2Fe_{16}Mn$ as deuterium is introduced, the change of the lattice volume and the change of the electronic structure. If volume changes play the major role in determining the magnetic states upon deuteration, the application of high external pressure should force the deuterides back to having the magnetic properties of the parent compounds. If pressure does not have this effect one would expect that changes of the electronic structure play the major role. Application of 10 kbar of hydrostatic pressure is estimated to decrease the unit cell volume by $\sim 1\%$,[35] i.e., we can approach the volumes of the parent compounds within our pressure limits. Table I shows that the introduction of 1 D/f.u. leads to a volume increase of about 0.7% that is −7 kbar/D according to the above made assumption. This value is in perfect agreement with Ref. 36 and references therein where the approximate scale factor of −8 kbar per 1 hydrogen atom in $R_2Fe_{17}H_y$ was reported.

The temperature dependences of the low field (50 Oe) magnetization of $Ce_2Fe_{16}MnD_1$ and $Ce_2Fe_{16}MnD_{2.3}$ under pressure are shown in Figs. 6(a) and 6(b), respectively. Com-

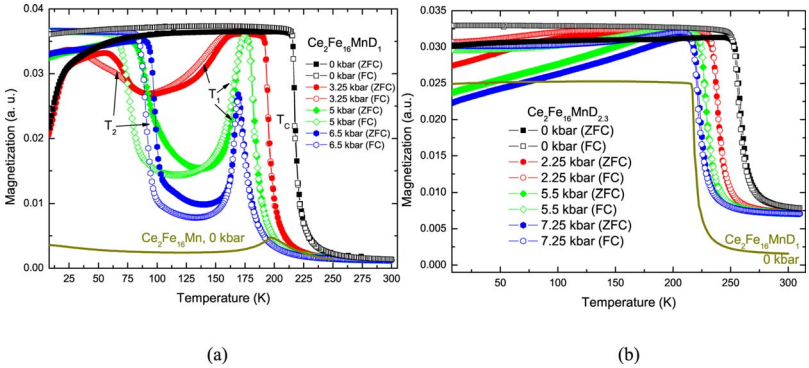

(a) (b)

FIG. 6. (Color online) Temperature dependence of the magnetization of $Ce_2Fe_{16}MnD_1$ (a) and $Ce_2Fe_{16}MnD_{2.3}$ (b) measured at $H=50$ Oe under pressure in comparison with ambient pressure results on $Ce_2Fe_{16}Mn$ and $Ce_2Fe_{16}MnD_1$, respectively. ZFC and FC runs are marked by solid and open symbols, respectively.

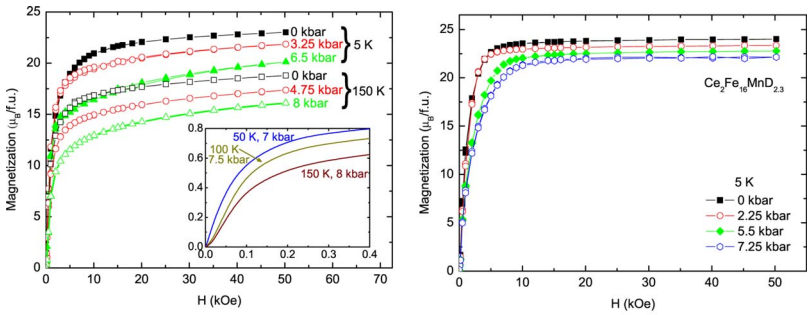

FIG. 7. (Color online) Magnetization isoterms of $Ce_2Fe_{16}MnD_1$ and $Ce_2Fe_{16}MnD_{2.3}$ under pressure.

paring the pressure evolution of the curves of $Ce_2Fe_{16}MnD_1$ with the one of $Ce_2Fe_{16}Mn$ at ambient pressure [Fig. 6(a)], one can see that they differ significantly even at the highest applied pressure of 6.5 kbar (5 K). The temperature dependence of the magnetization of $Ce_2Fe_{16}MnD_1$ under pressure is quite complex. It decreases with pressure and T_C shifts to lower values with $dT_C/dP=-5.4$ K/kbar. This value is about twice higher than the one in other compounds of this series,[10,31,32,34,37] but it is comparable to values obtained in R_2Fe_{17} intermetallic compounds (see, for instance, Refs. 38 and 39) and $Ce_2Fe_{17}H_y$ hydrides.[36,40] In the last, however, the application of high external pressure almost compensated the hydrogen induced magnetic anomalies.[36,40] With increasing pressure, the magnetization shows a wide dip at intermediate temperatures. Below the inflection point T_1 the magnetization decreases whereas the inflection point T_2 at lower temperatures marks its reincrease. With a further decrease of the temperature the curve becomes flat, reaching for the FC runs the value of the magnetization at 0 kbar (FC). The transitions look broad and smooth at low pressures but become more abrupt and narrower with increasing pressure. This peaklike anomaly of the magnetization curves for $P \geqslant 5$ kbar can be either considered as reflecting the narrow existence range of a ferromagnetic phase or as a peak reflecting a Néel temperature. From the pressure evolution of the magnetization curves, it looks that we deal most likely with the first situation where pressure suppresses the FM state at intermediate temperatures shifting simultaneously its transition to lower temperatures. Therefore all the transition temperatures (T_C, T_1, and T_2) were determined as inflection points of the corresponding curves.

Figure 7(a) presents the pressure effect on the magnetization isotherms of $Ce_2Fe_{16}MnD_1$ at 5 and 150 K. The magnetization significantly decreases under pressure and, simultaneously, the value of high field susceptibility increases. The last effect does not allow us to determine the pressure dependence of the saturation magnetization. Instead, we calculate the pressure induced decrease of the magnetization at maximum available field $M(50\ \text{kOe})$: $dM(50\ \text{kOe}, 5\ \text{K})/dP \approx -0.44\ \mu_B/\text{f.u. kbar}^{-1}$. We also cannot compare the increase of the magnetization in $Ce_2Fe_{16}MnD_1$ in comparison to the parent $Ce_2Fe_{16}Mn$ compound because the magnetization of the later is far from saturation even in 50 kOe (Fig. 3). The low field metamagnetic transitions present below 50 K and ambient pressure are suppressed at $P \geqslant 5$ kbar. Instead, metamagnetic transitions with low critical fields ($\sim$200 –300 Oe) are observed in magnetization isotherms at $P \geqslant 5$ kbar above 50 K [Fig. 7(a)]. This is in agreement with the dip present between T_1 and T_2 in the magnetization under pressure as shown in Fig. 6(a).

We can deduce from these magnetization measurements that pressure has a dual effect on the magnetic properties of $Ce_2Fe_{16}MnD_1$. At low temperatures pressure seems to suppress the AFM phase in favor of a FM ground state [suppression of the metamagnetic transition as shown by insert in Fig. 7(a)]. At intermediate temperatures, however, it acts contrary; the magnetization goes down and the temperature stability region of the FM phase narrows. It is not clear which kind of phase is realized between T_1 and T_2. According to the field dependence of the magnetization under maximum applied pressure of 6.5 kbar [Fig. 7(a)], the critical fields of metamagnetic transitions presented in between T_1 and T_2 are very low. This could mean that we are again in the presence of the AFM structure with very small propagation vector as seen at ambient pressure at low temperatures. A second possibility would be that pressure simply destroys long range FM order favoring the short range one. The last effect looks more probable as it excludes opposite effects of pressure at low and intermediate temperatures.

The effect of pressure on the magnetization curves of $Ce_2Fe_{16}MnD_{2.3}$ looks much simpler. A decrease of the magnetization with pressure and a change of T_C with $dT_C/dP=-3.6$ K/kbar [Fig. 6(b)] can be observed. Furthermore, one can see that the difference between the ZFC and FC curves increases with increasing pressure. Having in mind that this difference is caused by short range magnetic clusters we can suppose that high pressure induces this short range magnetic ordering at the cost of the long range FM one. This would be in agreement with the above made suggestion that the pressure induced magnetic phase between T_1 and T_2 in $Ce_2Fe_{16}MnD_1$ is of short range order. The similarity between the pressure induced magnetization curves of $Ce_2Fe_{16}MnD_{2.3}$ with the ones of $Ce_2Fe_{16}MnD_1$ at ambient pressure [Fig. 6(b)] indicates that the magnetic properties of the compounds with higher D content are determined mainly by volume changes. This observation qualitatively coincides with the one made for $Ce_2Fe_{17}H_y$ hydrides.[23,24,36,40] Comparing $Ce_2Fe_{16}MnD_{2.3}$ and $Ce_2Fe_{16}MnD_1$, one can find that ratio dT_C/dP recalculated per amount of inserted D is not constant in contrast to $Ce_2Fe_{17}H_y$. This confirms that deuterides with low D content are exceptional and their magnetic properties cannot be simply addressed to the volume increase.

Figure 7(b) visualizes the effect of high pressure on the field dependence of the magnetization of $Ce_2Fe_{16}MnD_{2.3}$. Contrary to $Ce_2Fe_{16}MnD_1$, saturation is reached at relatively small field values in $Ce_2Fe_{16}MnD_{2.3}$. The magnetization decreases under pressure with $dM(50\ \mathrm{kOe}, 5\ \mathrm{K})/dP \approx -0.24\ \mu_B/\mathrm{f.u.\ kbar}^{-1}$. This value is comparable with that of binary R_2Fe_{17} compounds[41] while it is approximately half the one obtained above for $Ce_2Fe_{16}MnD_1$. The observed pressure induced decrease of magnetization for $Ce_2Fe_{16}MnD_{2.3}$ is also close to a calculated value $\Delta M(50\ \mathrm{kOe}, 5\ \mathrm{K})/\Delta P \approx -0.18\ \mu_B/\mathrm{f.u.\ kbar}^{-1}$, where ΔM is difference between $M(50\ \mathrm{kOe}, 5\ \mathrm{K})$ for $Ce_2Fe_{16}MnD_{2.3}$ and $Ce_2Fe_{16}MnD_1$ at ambient pressure (Fig. 3) and ΔP is estimated from the difference in volume between $Ce_2Fe_{16}MnD_{2.3}$ and $Ce_2Fe_{16}MnD_1$ at 5 K assuming that ~1% of volume change is induced by a pressure of 10 kbar. This small difference in magnitudes of observed and calculated $dM(50\ \mathrm{kOe}, 5\ \mathrm{K})/dP$ supports the earlier made conclusion that the magnetic properties of $Ce_2Fe_{16}MnD_{2.3}$ are mainly determined by a volume effect. Contrary to this, the much higher value of $dM(50\ \mathrm{kOe}, 5\ \mathrm{K})/dP$ in $Ce_2Fe_{16}MnD_1$ pointed to the presence of another large contribution — obviously, the contribution resulting from deuterium induced changes of the electronic band structure.

IV. SUMMARY AND CONCLUSIONS

In this paper we presented the effects of D insertion (1, 2.3 D/f.u.) on magnetostructural properties of $Ce_2Fe_{16}Mn$ compound and influence of high pressures on magnetic properties of studied deuterides. The obtained results can be summarized as following:

(i) Deuteration of $Ce_2Fe_{16}Mn$ with up to 2.3 D/f.u. does not change the crystallographic structure type of the parent compound. Deuterium atoms are located in the 9*e* site of *R*-3*m* space group. Such a location gives a pronounced expansion of the lattice along *a* direction whereas the *c* parameter only slightly varies with increasing D content.

(ii) In general, insertion of deuterium into the lattice of AFM $Ce_2Fe_{16}Mn$ (application of negative chemical pressure) favors a ferromagnetic state of deuterides. Magnetic moments of both $Ce_2Fe_{16}MnD_1$ and $Ce_2Fe_{16}MnD_{2.3}$ align parallel to each other in the basal plane below $T_C = 218$ K and $T_C = 258$ K, respectively. Insertion of only 1 D/f.u., however, is not enough to keep $Ce_2Fe_{16}MnD_1$ ferromagnetic down to the lowest temperatures in contrast to $Ce_2Fe_{16}MnD_{2.3}$. $Ce_2Fe_{16}MnD_1$ undergoes a transition to AFM below ~40 K (Fig. 2). The AFM ground state is very unstable so small external field or further deuteration easily suppresses it.

(iii) Thermal behavior of the lattice of $Ce_2Fe_{16}MnD_y$ compounds ($y = 0, 1, 2.3$) is highly anisotropic, lattice contracts in *a* direction on cooling but at the same time anomalously expands in *c* direction. Magnetic anomalies presented in temperature behavior of the magnetization are clearly reflected in the thermal behavior of the lattice.

(iv) Application of (positive) high hydrostatic pressure leads to the decrease of both magnetization and transition temperatures with $dT_C/dP = -5.4$ K/kbar and $dT_C/dP = -3.6$ K/kbar for $Ce_2Fe_{16}MnD_1$ and $Ce_2Fe_{16}MnD_{2.3}$, respectively. Temperature evolutions of magnetization of $Ce_2Fe_{16}MnD_1$ and $Ce_2Fe_{16}MnD_{2.3}$ under pressure are different. The first involves appearance of the pressure induced magnetic phases while the second simply tends to the magnetization of $Ce_2Fe_{16}MnD_1$ at ambient pressure. The pressure induced decrease of magnetization for $Ce_2Fe_{16}MnD_1$ is also higher in comparison with that of $Ce_2Fe_{16}MnD_{2.3}$ and R_2Fe_{17} compounds.

(v) Obtained results clearly indicate that the ferromagnetic state in compounds with small D content ($Ce_2Fe_{16}MnD_1$) cannot be induced by changes of volume alone. Significant contribution from the modified electronic band structure is expected. However, further increase of D content ($Ce_2Fe_{16}MnD_{2.3}$) has a volume effect as dominating in observed magnetization behavior. Revealed phenomena suppose that electronic band structure calculations are highly desirable for complete understanding of magnetic properties of AFM $Ce_2Fe_{17-x}Mn_x$ compounds with $0.5 \leqslant x < 1.3$ and their deuterides.

ACKNOWLEDGMENTS

The financial support of AS CR within the Project No. AV0Z10100521, GA AS CR within the Project No. A1010315, RFBR within Grant No. 05-02-17244 and of CNRS-ASRT cooperation program #18115 is acknowledged.

[1] Y. Wang, F. Yang, N. Tang, C. Chen, and Q. Wang, J. Magn. Magn. Mater. **167**, 237 (1997).
[2] Z. Sun, H. Zhang, J. Wang, and B. Shen, J. Appl. Phys. **86**, 5152 (1999).
[3] P. C. Ezekwenna *et al.*, J. Appl. Phys. **81**, 4533 (1997).
[4] Y. Wang, F. Yang, C. Chen, N. Tang, P. Lin, H. Xiong, and Q. Wang, J. Magn. Magn. Mater. **185**, 339 (1998).
[5] M. Ellouze, Ph. L'Heritier, and A. Cheikh-Rouhou, Phys. Status Solidi A **179**, 423 (2000).
[6] T. H. Jacobs, K. H. J. Buschow, G. F. Zhou, J. P. Liu, X. Li, and F. R. de Boer, J. Magn. Magn. Mater. **104–107**, 1275 (1992).
[7] J. L. Wang *et al.*, J. Appl. Phys. **92**, 1453 (2002).
[8] R. C. O'Handley, *Modern Magnetic Materials: Principles and Applications* (Wiley, New York, 2000).
[9] D. Givord and R. Lemaire, IEEE Trans. Magn. **Mag-10**, 109 (1974).
[10] I. Medvedeva, Z. Arnold, A. Kuchin, and J. Kamarád, J. Appl. Phys. **86**, 6295 (1999).
[11] O. Prokhnenko, C. Ritter, Z. Arnold, O. Isnard, J. Kamarád, A. Pirogov, A. Teplykh, and A. Kuchin, J. Appl. Phys. **92**, 385 (2002).
[12] A. G. Kuchin, A. N. Pirogov, V. I. Khrabrov, A. E. Teplykh, A. S. Ermolenko, and E. V. Belozerov, J. Alloys Compd. **313**, 7 (2000).
[13] A. G. Kuchin, N. I. Kourov, Yu. V. Knyazev, N. M. Kleinerman, V. V. Serikov, G. V. Ivanova, and A. S. Ermolenko, Phys. Met. Metallogr. **79**, 61 (1995).
[14] Yu.V. Knyazev, A. G. Kuchin, and Y. I. Kuz'min, J. Alloys Compd. **327**, 34 (2001).
[15] D. P. Middleton, S. R. Mishra, G. L. Long, O. A. Pringle, Z. Hu, W. Yelon, F. Grandjean, and K. H. J. Buschow, J. Appl. Phys. **78**, 5568 (1995).
[16] M. Artigas, D. Fruchart, O. Isnard, S. Miraglia, and J. L. Soubeyroux, J. Alloys Compd. **270**, 28 (1998).
[17] M. Artigas, D. Fruchart, O. Isnard, S. Miraglia, and J. L. Soubeyroux, J. Alloys Compd. **291**, 282 (1999).
[18] S. R. Mishra, G. L. Long, O. A. Pringle, D. P. Middleton, Z. Hu, W. Yelon,

F. Grandjean, and K. H. J. Buschow, J. Appl. Phys. **79**, 3145 (1996).
[19]Z. Arnold, O. Prokhnenko, I. Medvedeva, A. Kuchin, and J. Kamarád, J. Magn. Magn. Mater. **226–230**, 950 (2001).
[20]O. Prokhnenko, C. Ritter, Z. Arnold, O. Isnard, A. Teplykh, J. Kamarád, A. Pirogov, and A. Kuchin, Appl. Phys. A: Mater. Sci. Process. **74**, S610 (2002).
[21]S. A. Nikitin, I. S. Tereshina, N. Yu. Pankratov, D. O. Louchev, G. S. Burkhanov, A. G. Kuchin, W. Iwasieczko, and H. Drulis, J. Alloys Compd. **365**, 80 (2004).
[22]W. Iwasieczko, A. G. Kuchin, and H. Drulis, J. Alloys Compd. **392**, 44 (2005).
[23]O. Isnard, S. Miraglia, D. Fruchart, C. Giorgetti, S. Pizzini, E. Dartyge, G. Krill, and J. P. Kappler, Phys. Rev. B **49**, 15692 (1994).
[24]J. L. Soubeyroux, D. Fruchart, O. Isnard, S. Miraglia, and E. Tomey, J. Alloys Compd. **219**, 16 (1995).
[25]J. Kamarád, Z. Machátová, and Z. Arnold, Rev. Sci. Instrum. **75**, 5022 (2004).
[26]J. Rodriguez-Carvajal, Physica B **192**, 55 (1993).
[27]K. H. J. Buschow, Rep. Prog. Phys. **40**, 1179 (1977).
[28]O. Isnard, S. Miraglia, J. L. Soubeyroux, D. Fruchart, and A. Stergiou, J. Less-Common Met. **162**, 273 (1990).
[29]O. Isnard, J. L. Soubeyroux, S. Miraglia, D. Fruchart, L. M. Garcia, and J. Bartolome, Physica B **180–181**, 629 (1992).
[30]A. V. Andreev and A. Lindbaum, J. Alloys Compd. **297** 43 (2000).
[31]O. Prokhnenko, Z. Arnold, I. Medvedeva, A. Kuchin, and J. Kamarád, Low Temp. Phys. **27**, 275 (2001) [Fiz. Nizk. Temp. **27**, 375 (2001)].
[32]O. Prokhnenko, Z. Arnold, J. Kamarád, C. Ritter, O. Isnard, and A. Kuchin, J. Appl. Phys. **97**, 113909 (2005).
[33]D. Gignoux, D. Givord, F. Givord, and R. Lemaire, J. Magn. Magn. Mater. **10**, 288 (1979).
[34]O. Prokhnenko, Ph.D. thesis Charles University (2003).
[35]Z. Arnold, M. R. Ibarra, L. Morellon, P. A. Algarabel, and J. Kamarád, J. Magn. Magn. Mater. **157–158**, 81 (1996).
[36]S. Niziol, R. Zach, M. Bacmann, D. Fruchart, O. Isnard, S. Miraglia, and J. L. Soubeyroux, J. Alloys Compd. **262–263**, 202 (1997).
[37]A. G. Kuchin, I. V. Medvedeva, V. S. Gaviko, and V. A. Kazantsev, J. Alloys Compd. **289**, 18 (1999).
[38]M. Brouha and K.H. J Buschow, J. Appl. Phys. **44**, 1813 (1973).
[39]J. J. M. Franse and R. J. Radwanski, *Handbook of Magnetic Materials*, edited by K.H. J. Buschow (Elsevier, New York, 1993), Vol. 7.
[40]O. Isnard, R. Zach, S. Niziol, S. Miraglia, and D. Fruchart, J. Magn. Magn. Mater. **140–144**, 1073 (1995).
[41]J. Kamarád, O. Mikulina, Z. Arnold, B. Garcia-Landa, and M. R. Ibarra, J. Appl. Phys. **85**, 4874 (1999).